6-22-2004

Radical Initiated Polymerization In a Bifunctional Mixture Via Computer Simulation

Keri L. Diamond
University of Southern Mississippi

Ras B. Pandey
University of Southern Mississippi, ras.pandey@usm.edu

Shelby F. Thames
University of Southern Mississippi, Shelby.F.Thames@usm.edu

Radical initiated polymerization in a bifunctional mixture via computer simulation

Keri L. Diamond
School of Polymers and High Performance Materials, University of Southern Mississippi, Hattiesburg, Mississippi 39406

Ras B. Pandey[a)]
Department of Physics and Astronomy, University of Southern Mississippi, Hattiesburg, Mississippi 39406

Shelby F. Thames
School of Polymers and High Performance Materials, University of Southern Mississippi, Hattiesburg, Mississippi 39406

(Received 12 February 2004; accepted 31 March 2004)

Computer simulations are performed to study the polymerization behavior in a mixture of bifunctional groups such as olefins (A) and acrylates (B) in an effective solvent (a coarse description for vegetable oil derived macromonomers (VOMMs) in solution) on a cubic lattice. A set of interactions between these units and solvent (S) constituents and their relative concentrations (p_A, p_B, and p_S) are considered. Samples are equilibrated with Metropolis algorithm to model the perceived behavior of VOMMs. The covalent bonding between monomeric units is then implemented via reaction pathways initiated by stochastic motion of free radicals (a very small fraction). The rate of reaction shows decay patterns with the time steps (t) with power laws (i.e., $R_{ab} \alpha t^{-r}$, $r \cong 0.4-0.8$), exponential decays (i.e., $R_{ab} \alpha e^{-0.001t}$), and their combination. Growth of A–B bonding is studied as a function of polymer concentration $p = p_A + p_B$ for four different model systems appropriate for VOMMs. The data from the free radical initiated simulations are compared to the original simulations with homopolymerization. While most of the data are consistent with experimental observations, the variations are found to be model dependent. © *2004 American Institute of Physics.* [DOI: 10.1063/1.1753564]

I. INTRODUCTION

Vegetable oil derived macromonomers (VOMMs) are incorporated into emulsion polymers and employed as coalescing aids, replacing volatile organic solvents (VOCs) that are currently being used. Once the film is applied, property development occurs via auto-oxidation of unsaturation found along the backbone of the oil, thus forming a crosslinked network.[1] The technology is an environmentally friendly alternative to the traditional high-VOC products that currently dominate the market.

It is speculated that both proximity of the polymerizable group to the sites of unsaturation along the oil backbone and the ratio of acrylates to olefins, play a major role in the incidence of chain transfer. Polymerization[2] via pendent acrylate functionalities facilitates the incorporation of the VOMMs into the polymer backbone. The challenge is the preservation of the allylic double bonds during the free-radial polymerizations. Allylic hydrogens are highly susceptible to chain transfer reactions, which results in low conversion, high gel content, and branching.[3] It has been shown via nuclear magnetic resonance that the mechanism of chain transfer can be one of the two possibilities (Figs. 1 and 2). Intramolecular chain transfer via proton abstraction is shown in Fig. 1. Polymerization through the oil double bonds (Fig. 2) is another side reaction that reduces the unsaturation in the polymer and limits the potential for oxidative cure post application.[4]

Many computer simulations have been performed to model polymerizations[5–13] in recent years, but there are relatively few that have modeled specific systems. This study is an attempt to model the free-radical polymerization of VOMMs in a solution. This model employs phenomenological interactions as a means of equilibrating the distribution of neighboring functional groups. Unlike previous computer simulations,[14] where each monomeric unit reacts with their nearest neighbors (an effective medium homopolymerization), a radical initiated polymerization is considered to bring it closer to a realistic representation of the experimental systems. In free-radical polymerization, covalent bonds are formed along the trails of kinetic reaction pathways of mobile radicals. Simulations were performed at various polymer concentrations with different fractions of acrylate–olefin ratios appropriate for laboratory systems. Results are compared to the original data generated via homogeneous polymerization.

II. MODEL AND METHOD

Particles of molecular weight M_A and M_B represent olefins (A) and acrylates (B) on a cubic lattice of size L^3 with each particle occupying a lattice site. The volume fractions p_A and p_B of particles A and B constitute the polymer con-

a)Electronic mail: ras.pandey@usm.edu

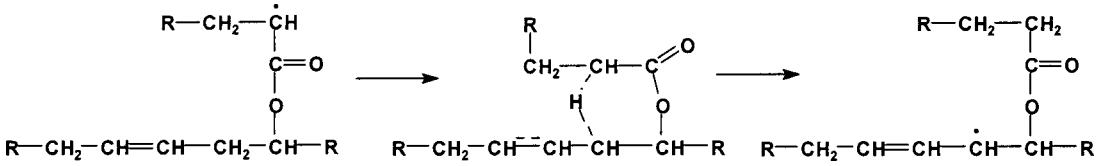

FIG. 1. Proton abstraction reaction.

centration $p=p_A+p_B$. Initially, particles A and B are randomly distributed (only one particle at a site). The fraction of empty sites $p_S=1-p$ represents the effective solvent concentration. A set of nearest-neighbor interactions between particles A, B, and solvent (S) sites are used to equilibrate their relative distribution and mobility, in order to describe appropriate VOMM mixtures with different structural constituents.[14] For example, a typical phenomenological interaction energy (E) in arbitrary units is given by

$$E_{AA}=E_{BB}=-1, E_{AB}=-2. \tag{1}$$

Accordingly, the proximity of A to B is relatively more favorable than the proximity of A to A or B to B, which are desired features hypothesized for a set of experimental systems.[3,4] Another possible interaction is

$$E_{AA}=E_{AB}=-1, E_{BB}=-2. \tag{2}$$

This enhances the probability of B surrounded by B in comparison to A or B surrounded by A. The experimental system[3,4] is thus represented (approximately) by interactions set like Eqs. (1) and (2) among the functional groups along with their concentrations (p_A,p_B). The quality of solvent is controlled by a nearest-neighbor interaction between the functional units (A, B) and the solvent sites,

$$E_{AS}=E_{BS}=-1. \tag{3}$$

The sample is equilibrated[14] by moving each functional group for a sufficiently long time with the Metropolis algorithm, implemented by the following method. A particle—A or B—at site i and one of its neighboring sites, j, are selected randomly. If site j is empty, then an attempt is made to move the particle from site i to j with a Boltzmann distribution,

$$\exp\left(\frac{-\Delta E}{k_B \cdot T}\right), \tag{4}$$

where T is the temperature and ΔE is the change in the energy of the particle if it were to move to site j. Periodic boundary conditions are used along the x, y, and z directions. An attempt to move each particle once defines a unit Monte Carlo Step time. The sample is equilibrated for a sufficiently long time by monitoring the steady-state values of the energy and visualization of the structural patterns.

Polymerization is then initiated by stochastic motion of randomly distributed radicals from a monomer at site, say i, to a randomly selected neighboring monomer at site j. Attempts are made to form a covalent bond between the two sites (i, j) with probability $k_{\alpha,\beta}$, if both have at least one unsaturated bond. However, if both sites (i, j) have radicals, then these two radicals annihilate each other, but the bond is still formed if they have unsaturation. Thus, the covalent bonds grow on the trail of the radical movements (from one monomer to another). In one time step, movement of all unreacted monomers (A,B) is followed by radicals' move and reaction with a probability $k_{\alpha,\beta}$. Note that a radical is also carried by stochastic motion of an unreacted host monomer from one site to another. However, once the monomer is immobilized, it is still possible for radicals (including the one at this monomer) to move from one site to another only if a covalent bond results between the two sites. A functional group becomes saturated when both of its functionalities becomes part of a covalent bond. During the simulation, the growth of covalent bonds (A–B, B–B) and their relative fractions are monitored. Simulation is carried out for sufficient time steps for the conversion factor to reach a near constant value. To obtain a reliable estimate of the average conversion factors, the simulations are repeated for many independent samples each involving equilibration from an initial random distribution of constituents followed by polymerization. Simulations are carried out on different lattice sizes, however, most of our data presented here are generated on a 50^3 lattice as no significant finite size effects are noticed on the qualitative behavior of bond formations. The statistical error bars are within the size of symbols used in the figures. In the following section, four specific systems based on interactions [Eqs. (1)–(3)] and appropriate concentration ratios $p_A/p_B=1$, $p_A/p_B=5$ and $p_A/p_B=2$ are considered.

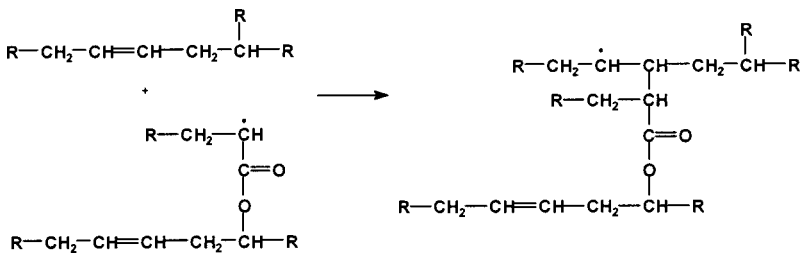

FIG. 2. Addition across allylic double bonds.

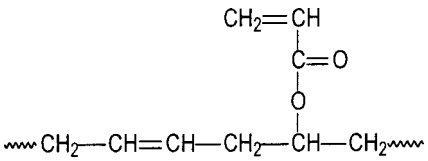

FIG. 3. Acrylate positioned directly off the backbone.

III. SIMULATION CONDITIONS

Based on laboratory experiments,[2,3] a reaction between two olefins (A–A) is relatively less likely during the polymerization, therefore, A–A bonding is not considered. The kinetic reactions between the olefins (A) and acrylates (B), for example, is described by reaction probabilities: $k_{BB}=k_{AB}=0.25$, $k_{AA}=0$. Thus, bonds are allowed to form with a 25% probability when a radical from a site i occupied by a B group attempts to move to a neighboring site j occupied by A or B. Polymerization only occurs between A–B, or B–B subject to availability of unreacted functionalities of reacting units.

The growth fraction of B–B, and A–B bonds, is determined for four different systems. Each system represents the overall configurational characteristics of a VOMM with respect to their proximity, mobility, and relative concentrations. (i) For the acrylate positioned directly off the backbone, as in Fig. 3, the proximity of the olefins (A) to acrylates (B) is described by the interaction energy [Eqs. (1) and (3)] and concentration (or volume fraction) ratio of [A]:[B] is 1:1 ($p_A/p_B=1$). (ii) The acrylates (B) and the olefins (A) are separated by a spacer linkage R as shown in Fig. 4. The interactions [Eqs. (2) and (3)] and their fractional ratio of [A]:[B] is 5:1 ($p_A/p_B=5$). Interaction between groups (A, B) is identical to that in system (ii) but with concentration ratios of [A]:[B]=2:1 ($p_A/p_B=2$), in system (iii), and [A]:[B] ratio of 1:1 in system (iv).

IV. RESULTS AND DISCUSSION

As described above, the olefins (A), acrylates (B), and solvent (S) are randomly dispersed on the cubic lattice initially. However, the mixture is brought to a thermodynamic equilibrium (Fig. 5) prior to reaction initiation. The approach to thermodynamic equilibrium is determined by monitoring the interaction energy with time steps. After radical initiation, the polymerization occurs very fast until saturation is reached. A typical snapshot of the distribution of functional groups and bond growth is shown in Fig. 6.

The free radical initiated polymerizations are found to have greater chain transfer events (A–B bonding) (see below) since the polymerization occurs via reaction pathways, creating greater heterogeneities throughout the lattice.

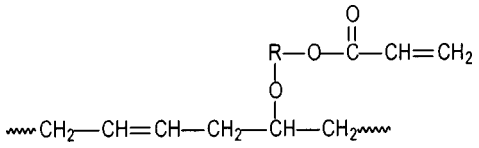

FIG. 4. Acrylate positioned R-carbons away from the backbone.

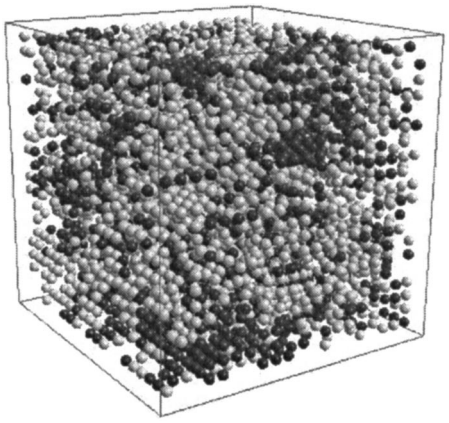

FIG. 5. Snapshot of an equilibrated system prior to reaction initiation. A (dark), B (light) spheres on a 30^3 lattice for system (ii).

Variation of the AB bond with time for systems i–iv with polymer concentration $p=0.5$ and 0.7 is presented in Fig. 7. It is easy to note that the growth of bonds is neither linear nor a power law with time steps. However, the population of AB bonds grow rapidly during the initial stage of reaction followed by a slow increase. Further, the growth varies with the system (i–iv) and depends on the polymer concentration ($p=0.5$, 0.7). Thus, the bond growth is specific to systems.

In an attempt to find an empirical relation for the bond growth, the rate of reaction is examined in detail. The rate of polymerization for each simulation is determined by evaluating the rate of bond growth as a function of time steps (see Fig. 8). It is rather difficult to identify a universal decay law (i.e., exponential, power law, etc.) that can fit with all of the data sets. However, systems (ii) and (iii) seem to exhibit distinct decay features with some clarity (see insets of Fig. 8); both systems have the lowest ratio of acrylates to olefins.

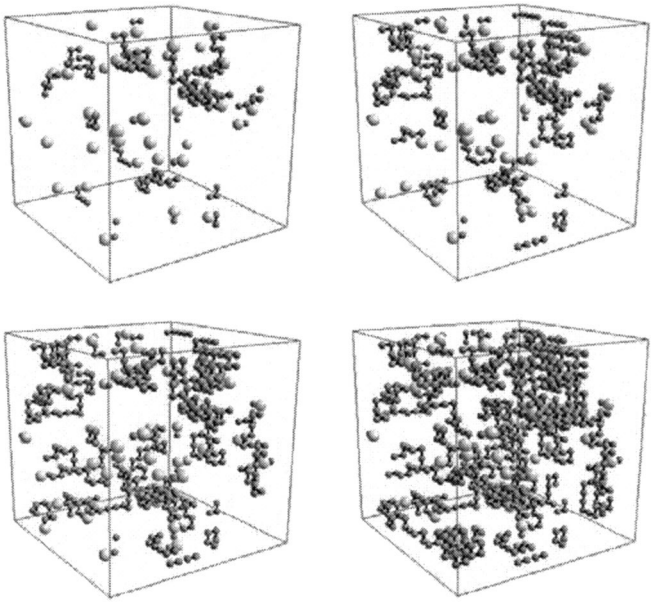

FIG. 6. Typical snapshot of the distribution of reacted functional groups and bond growth at times steps ($t=10$, 30, 50, and 100) after equilibration (for 500 time steps) on a 30^3 lattice. The large spheres represent radicals.

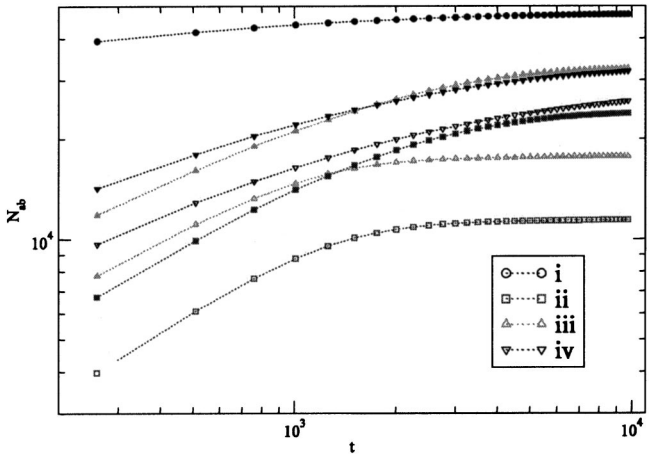

FIG. 7. Number of AB bonds vs time (t) steps on a 50^3 sample with ten independent runs and radical concentration $p_r=0.01$ at polymer concentration $p=0.5$ (open) and 0.7 (filled).

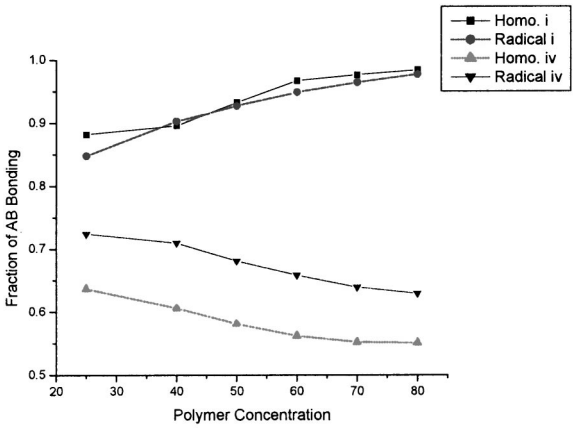

FIG. 9. Fraction of saturated AB bonds versus total polymer concentration for $k_{AA}=0$, $k_{AB}=k_{BB}=0.25$ with equilibrated lattice (for 10^4 time steps) prior to reaction initiation, sample size 50^3 with ten independent at each polymer concentration with radical concentration ($p_r=0.01$). Data for homogeneous polymerization are included for comparison.

The lower inset of Fig. 8 suggests power-law decays for the rate of reaction, i.e.,

$$R_{ab}\alpha t^{-0.4}(\text{ii}),\ \ R_{ab}\alpha t^{-0.6}(\text{iii}) \tag{5}$$

followed by

$$R_{ab}\alpha t^{-0.8}(\text{ii,iii}). \tag{6}$$

The log–normal fits of the data (upper inset of Fig. 8), on the other hand, shows a weak exponential decays just after initiation, i.e.,

$$R_{ab}\alpha e^{-0.0014t}(\text{ii}),\ \ R_{ab}e^{-0.0017t}. \tag{7}$$

It is hard to identify such rate of reaction decay laws from the long-time tails. Thus, the rate of reaction (R_{ab}) decays with a power-law $R_{ab}\alpha t^{-r}$ with an exponent r which shows a crossover from slow ($r=0.4$, 0.6) to a rapid decay ($r=0.8$) for systems (ii) and (iii). Data for systems (i, iv) seem to fall in between, possibly a rate of reaction decay with a combination of power law and exponential. To examine the effect of acrylate proximity to the backbone of the oil, a comparison is made between system (i), which represents a VOMM with an acrylate directly off the backbone of the oil, and system (iv), which represents a VOMM with the acrylate positioned away from the backbone. In system (i), the fraction of A–B bonding is over 85% and increases with polymer concentration, up to a maximum of 98% (see Fig. 9). The occurrence of chain transfer in system (iv) however, is significantly lower, starting at 64% at low polymer concentrations and decreasing to 55%.

The difference between the homogeneous polymerization and the free radical simulations varies from on system to another. In system (i), there is very little difference between the two simulations, however, there is significant variation in the simulations in system (iv) (Fig. 9). Once at equilibrium, the A's in system (i) are surrounded by B's, therefore the likelihood of A–B interaction is high under both homogeneous and heterogeneous (radical) polymerization conditions. Therefore, it is not particularly surprising that there is little difference between the two simulations. However, in

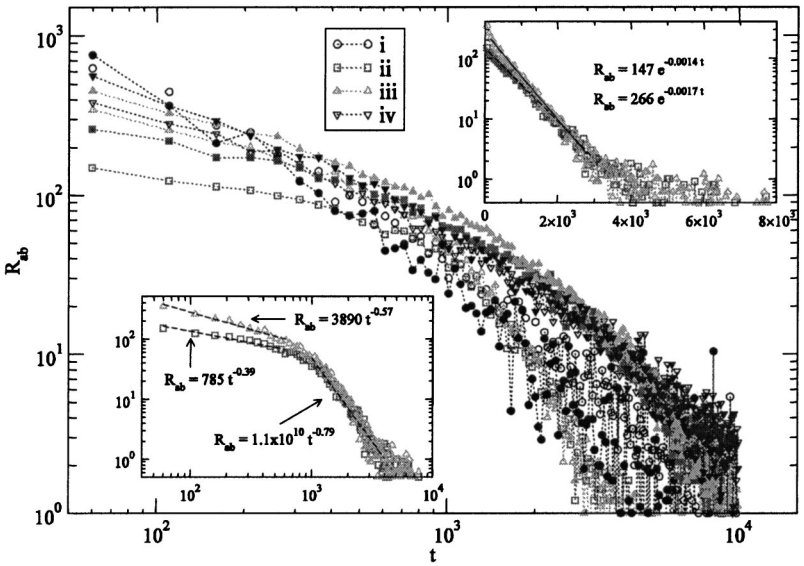

FIG. 8. Rate of reaction R_{ab} vs number of time steps at polymer concentrations $p=0.5$ (open) and 0.7 (filled) for each system (i–iv). Lattice of size 50^3 is used with ten independent runs for each system. Insets show some of the data on log–log (lower left-hand side) and log–normal (upper right-hand side) scales for clarity to identify the trends.

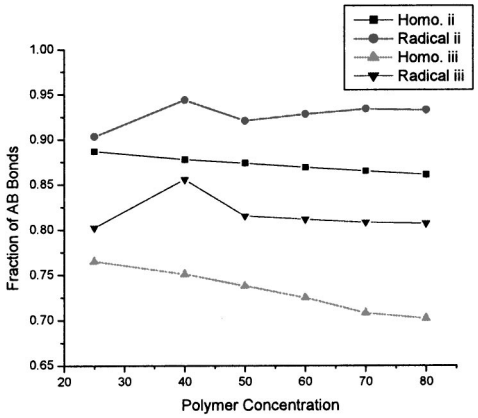

FIG. 10. Fraction of saturated AB bonds vs polymer concentration for $k_{AA}=0$, $k_{AB}=k_{BB}=0.25$ with equilibrated lattice (for 10^4 time steps) prior to reaction initiation, sample size 50^3 with ten independent runs for system ii and iii at each polymer concentration.

system (iv), after the equilibrium, B's are likely to be next to each other creating aggregates of B's throughout the lattice, see Fig. 5. The darker spheres represent the acrylates in the system. During heterogeneous (radical initiated) polymerization, the reaction occurs via a limited number of reaction centers (radicals) along a random one-dimensional path that can drift away from the B clusters into areas with higher concentrations of A. This reduces the likelihood of a B–B reaction. In contrast, when polymerization occurs in an isotropic manner throughout the entire lattice, the likelihood of a B–B interaction is maximized (see Fig. 10).

A similar effect is seen when a comparison is made between the homogeneous and radical initiated polymerizations of system (ii) and (iii). Both systems have strong B–B interactions, however, the ratio of A:B is very different: 5:1 in (ii) and 2:1 in (iii) The lower concentration of B's in system (ii) result in smaller clusters, therefore there is not as great a difference between the homogeneous and heterogeneous polymerizations. In system (iii), the concentration of B's is higher, resulting in larger clusters and therefore a greater difference between the simulations.

V. SUMMARY AND CONCLUSIONS

A computer simulation is designed to mimic the polymerization behavior of VOMMs in solutions. Olefins (A), acrylates (B), and an effective solvent (S) are distributed and equilibrated throughout a cubic lattice at various concentrations ($p=0.2$–0.8). Polymerization occurs along reaction pathways initiated by a low concentration ($p_r=0.01$) of free radicals. Four different systems are used in this study, each representing a different VOMM structure. The rate of polymerization as a function of time steps is analyzed. Both power-law and exponential decays of the rate of reaction seem to occur specifically in systems (ii) and (iii), with distinct regions.

The free-radical simulation data are compared to the original simulation with homogeneous polymerization.[14] The number of A–B bonds as a function of polymer concentration is determined for each system. Significant variations are found in the fraction of A–B bonds which depend on the ratio of acrylates to olefins and the proximity of the functional groups to each other. In systems where aggregates of acrylates were prevalent throughout the lattice (systems ii–iv), there is an increase in the number of A–B bonds as a function of polymer concentration. In system (i) however, few aggregates of acrylates develop during the equilibrium stage, and there is very little difference between free radical and homogeneous polymerizations.

ACKNOWLEDGMENTS

The authors would like to thank USDA/CSREES/NRICGP Agreement No. 2001-35504-10755, the MRSEC program of the National Foundation Agreement No. DMR-0213883, and NSF-EPSCOR Grant No. EPS-0132618 for financial support.

[1] S. F. Thames, *Proceedings of the 25th International Waterborne, High-Solids, and Powder Coatings Symposium* (1998), pp. 305–320.
[2] G. Odian, *Principles of Polymerization*, 3rd ed. (Wiley-Interscience, New York, 1991).
[3] E. H. Brister, O. W. Smith, and S. F. Thames, *Proceedings of the 26th International Waterborne, High-Solids, Powder Coatings Symposium* (1999), pp. 89–90.
[4] K. L. Diamond, S. N. Shah, O. W. Smith, and S. F. Thames, *Proceedings of the 30th International Waterborne, High-Solids, and Powder Coatings Symposium* (1998), pp. 305–320.
[5] F. Family and D. P. Landau, *Kinetics of Aggregation and Gelation* (North-Holland, New York, 1984).
[6] D. Staffer, A. Coniglio, and M. Adam, Adv. Polym. Sci. **41**, 103 (1982).
[7] H. J. Herrmann, Phys. Rep. **136**, 153 (1986).
[8] K. S. Anseth and C. N. Bowman, J. Polym. Sci., Polym. Phys. Ed. **33**, 1769 (1995).
[9] K. S. Anseth, L. M. Kline, T. A. Walker, K. J. Anderson, and C. N. Bowman, Macromolecules **28**, 2491 (1995).
[10] V. Patton, J. A. Wesson, M. Rubinstein, J. C. Wilson, and L. E. Oppenheimer, Macromolecules **22**, 1948 (1989).
[11] K. S. Anseth, L. M. Kline, T. A. Walker, K. J. Anderson, and C. N. Bowman, Macromolecules **28**, 2491 (1995).
[12] Y. Liu and R. B. Pandey, J. Chem. Phys. **105**, 825 (1996).
[13] R. B. Pandey and Y. Liu, J. Sol-Gel Sci. Technol. **15**, 147 (1999).
[14] K. L. Diamond, R. B. Pandey, and S. F. Thames, Struct. Chem. (to be published).